Neuromorphic Processing in Moving Sonar for Landmark Classification

Roman Kuc

Department of Electrical Engineering
Yale University, New Haven, CT, 06520-8284, USA
kuc@yale.edu

Abstract

Sonar uses echolocation to measure range to objects at low cost and computational effort. From range readings to landmark classification is large step, although bats and dolphins are successful at it. These biosonars move while scanning and we employ this strategy to classify objects. Our sonar generates a random pulse sequence related to echo waveform amplitude, which we term pseudo-action potentials (PAPs) because of their similarities to biological spikes. We employ neuromorphic elements, such as delays, threshold, coincidence detection, short-term memory, and massive parallelism to classify objects from their echoes. When the sonar moves along a linear trajectory, a small object produces hyperbolic range readings parameterized by the passing range. Estimates of the passing range form a temporal coincidence of the PAP arrival times. This talk demonstrates that features of range and passing-range data are useful for object classification.

1. Introduction

Sonar is a useful sensing modality for robotics, but the data produced by conventional time-of-flight (TOF) ranging sensors is difficult to interpret. Information for object recognition can be obtained by capturing the entire echo waveform [1, 2], rather that just the TOF, but analog-to-digital conversion can be expensive. As a less expensive approximation, our sonar converts a echo waveform into a random point process by repeatedly resetting a conventional detector [3]. These random points are called *pseudo-action potentials (PAPs)* because of their similarity to biological action potentials. The PAP temporal density relates to echo amplitude and allows strong echoes to be identified for processing. This paper describes how to process PAPs observed by a moving sonar to classify objects that can be used as landmarks for mobile robot navigation.

2. Sonar configuration

Figure 1 shows a ranging sensor moving along a linear trajectory in steps equal to Δy. The sequence of range

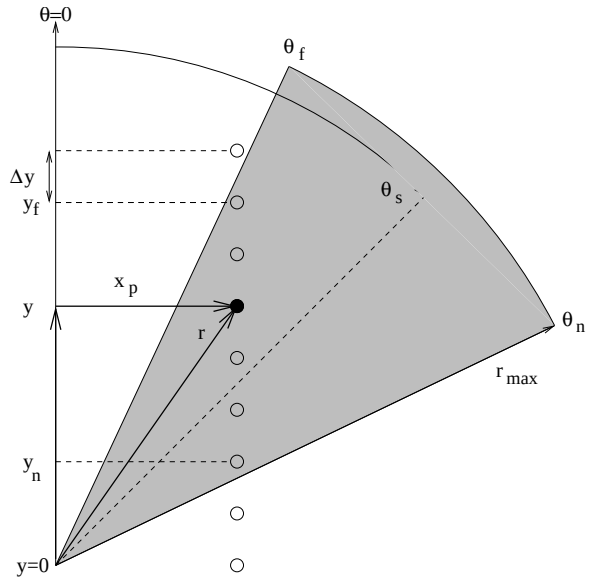

Figure 1: Sonar moving in the $\theta = 0$ direction with step size Δy past an object (circles show location sequence referenced to sonar position). Sonar axis is denoted θ_s with beam extending from θ_f to θ_n.

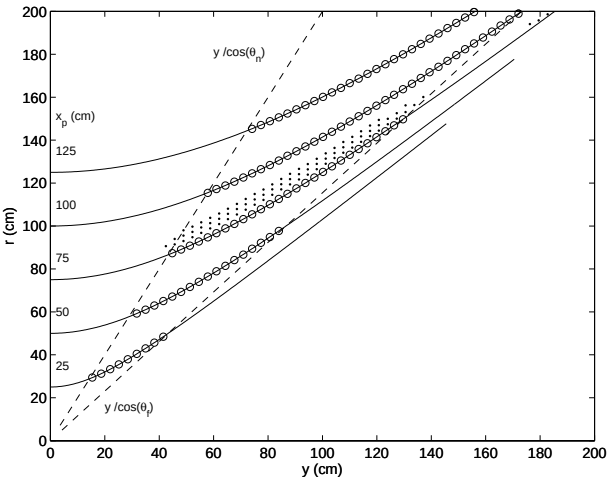

Figure 2: Hyperbolic range readings for different values of passing range x_p. PAPs from a 10 mm diameter post reflector with $x_p \approx 80$ cm are shown as dots.

measurements to a small object follows a hyperbola:

$$r_k = \sqrt{x_p^2 + (y_n + k\Delta y)^2} \quad (1)$$

for $k = 0, 1, \cdots, N-1$ where

- x_p is the *passing range*
- y_n is the sonar location producing r_o
- $N \approx \frac{y_f - y_n}{\Delta y} + 1$ is the number of readings observed.

The range measurements are *in reverse order* of the observations because they will be stored in short-term memory and processed shortly after the last one, r_0, is observed. The classification should be accomplished before the object location becomes y_n, or just before the object leaves the beam. Fig. 1 shows

$$y_n \approx \frac{x_p}{\tan(\theta_n)} \quad (2)$$

and

$$r\ \sin(\theta_f) \leq x_p \leq r\ \sin(\theta_n) \quad (3)$$

Figure 2 shows sets of range readings produced by a small object for different x_p values. Locating the object means determining x_p and y_n soon after r_o is observed. The conventional method is to use the values shown as templates, to cross-correlate these templates with the measurements and to find the template producing the maximum value. This is the optimal localization procedure for measurements in the presence of noise. However, the standard signal-in-additive-noise model is not appropriate for sonar range measurements since the sonar measurements are robust. Artifacts, such as reverberations, phase cancelation, TOF jitter, and side lobes are more troublesome, but will be accommodated by our neuromorphic processing.

This paper also considers PAPs reflected from a rough planar surface. When the sonar moves parallel to the surface the range readings have a mean value $\overline{r} \approx x_p / \sin(\theta_n)$ and a variance related to the surface roughness.

An interesting parameter for a mobile sonar is the passing range x_p since it determines if a collision is likely to occur. Eq. (1) provides N estimates of x_p

$$\hat{x}_p(k) = \sqrt{r_k^2 - (y_n + k\Delta y)^2} \quad (4)$$

We cannot solve for $\hat{x}_p$ directly because we do not know y_n. We previously found $\hat{x}_p$ and $\hat{y}_n$ by using the templates for a candidate pair and then performing a two-dimensional search in the (x_p, y_n) space to find the best least-squares fit [3].

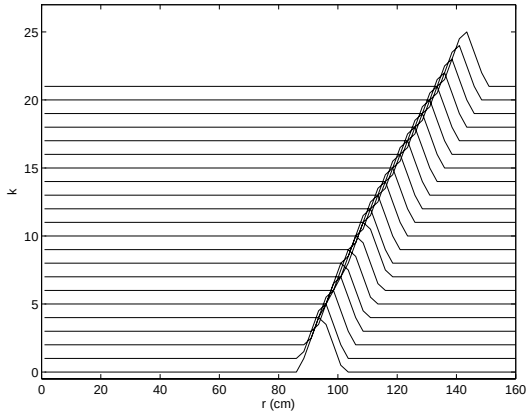

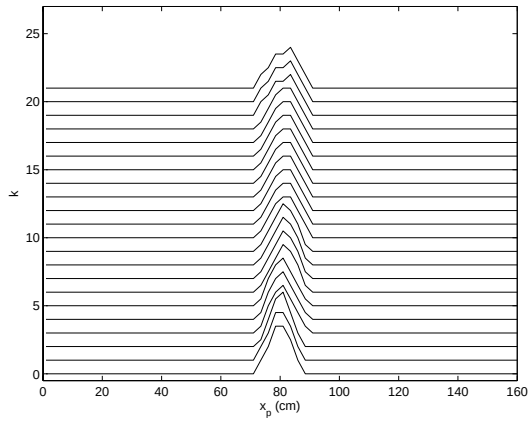

Figure 3: Post echo data in short-term memory. Most recent echo corresponds to $k = 0$. a) Range histogram of PAPs with $y_n = 46$ cm. b) Histogram of $\hat{x}_p(k)$ with $y_n = 46$ cm.

3. Neuromorphic processing

This paper considers a neuromorphic coincidence detection approach as an alternative to our previous off-line method. We illustrate this new method by applying it to range data observed by moving past a 10 cm diameter cylindrical post with $\Delta y = 3$ cm. We first extract the strong echoes from the PAP data by finding when three successive PAPs fall within a specified range interval (5 cm). We form a histogram of the strong echoes as a function of range, with results shown in Fig. 3a, corresponding to our set of range measurements. This step helps identify reverberation artifacts. We then apply Eq.(4) to estimate x_p from the set of r_k range measurements by assuming values for y_n, one for each detector. The detector with approximately the correct y_n value will cause the estimates to cluster around the true x_p value just as the last measurement r_o occurs. The results for the detector with $y_n = 46$ cm is shown in Fig. 3b. We identify this coincidence condition by summing the columns in the short-term memory and observing when its peak value is a maximum. A missing strong echo resets the

Figure 4: Image of doorway with adjacent window and cinder block objects.

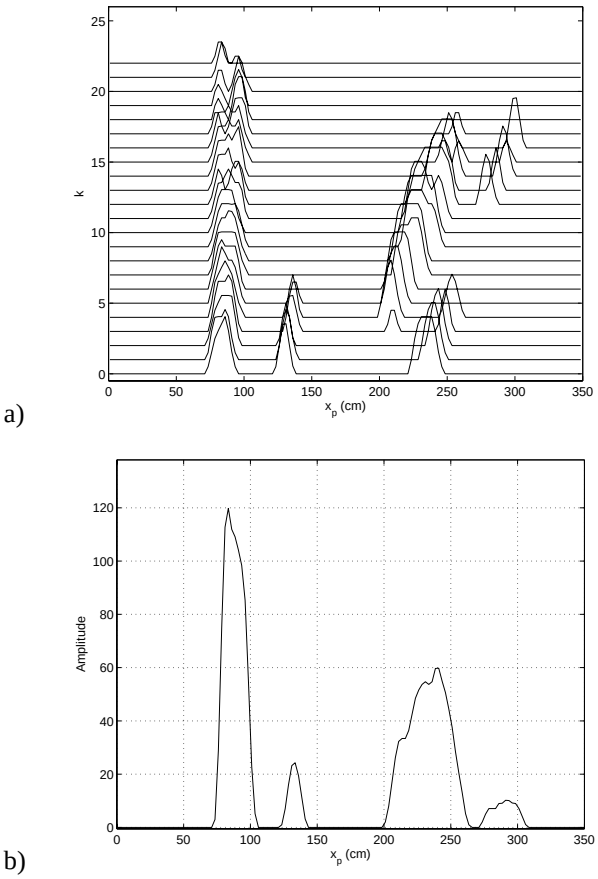

Figure 5: Doorway echo data. a) Short-term memory with estimates of x_p. b) Sum of memory columns when first peak is a maximum.

sum because the sonar range readings are robust. A suitably large threshold for the sum eliminates the echoes from the side lobes. The object is *perceived* when the peak sum passes through its maximum value. Only the detector with the approximate value of y_n exhibits such a peak in the sum.

4. Results with more complex objects

To acquire more typical data our sonar moved down a hallway composed of doorways in a cinder block wall, as shown in Fig. 4. The door and window jambs form a pair of strong retro-reflectors having the same x_p value, while the rough cinder block is a typical random surface. We applied the $\hat{x}_p$ estimation procedure to the hallway data with $y_n = 46$ cm.

Figure 5a shows the results when the peak of the column sum passes through a maximum. The expected coincidence in $\hat{x}_p$ occurs at $x_p = 85$ cm (close to the true value [3]) in the door jamb data and a smaller, but not-coincident, peak at a larger x_p value due to the window jamb data. The y_n value for the door jamb detector is also appropriate for the window jamb, because the two have the same x_p, but the r_o for the window jamb occurs a a later time, hence they would be coincident at a larger y value. At the time shown that makes the door jamb echoes coincident, the window jamb echoes are shifted to larger x_p values. This interesting feature allows close-by objects at the same passing range to be separated in x_p space. The maximum of peak is shown to occur in Fig. 5b. The double peak pattern, corresponding to the door and window jambs, is a useful landmark, which has been localized at $x_p = 80$ cm and $y_n = \sqrt{r_o^2 + x_p^2}$.

Figure 5 also shows additional data for $x_p > 200$ cm. These are caused by multiple reflection artifacts due to echoes bouncing off the detector and acting as secondary probing pulses. These artifacts are eliminated by limiting the echo analysis to twice the range of the first echoes, in this case approximately 160 cm.

Figure 6 shows the echoes from the cinder block surface for comparison. Since the echoes are not from a small object we would not expect the x_p estimates to be coincident and they are not. So we show only the more interesting PAP range histograms, which although they have a random variation also are coincident, with mean range $\overline{r} = 100$. In our experiments $\theta_n = 60^o$. The $x_p = 85$ cm results from the window and door jambs are in good agreement with the observed $\overline{r}$ value.

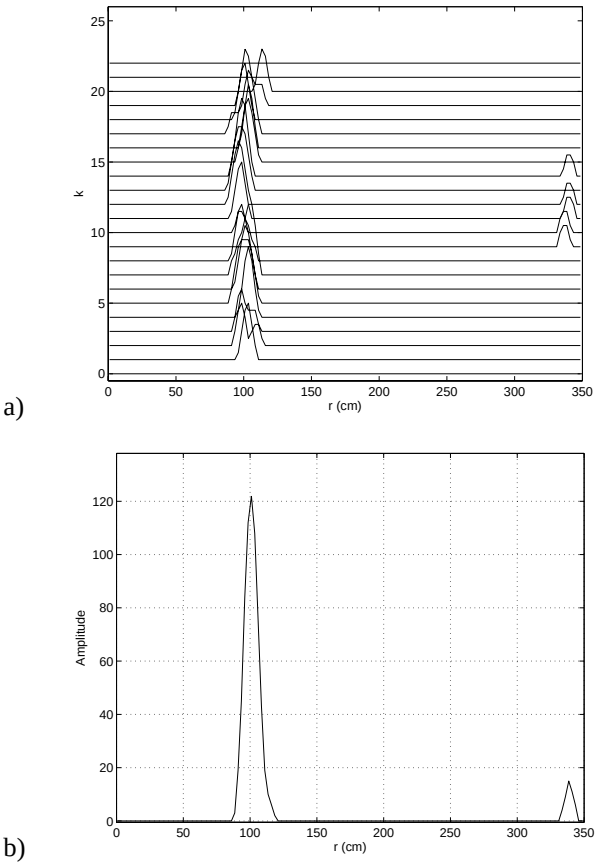

Figure 6: Cinder block echo data. a) Short-term memory containing histograms of r_k values. b) Sum of memory columns when first peak is a maximum.

5. Discussion

The results indicate that coincidence in short-term memory of both the range r_k and $\hat{x}_p$ values lead to classification of interesting object types. When a coincidence is observed in $\hat{x}_p$ the echo-producing object is small (compact) or a retro-reflector, both of which produce hyperbolic range readings when the sonar moves along a linear trajectory. Coincidence in r_k indicates the object is a rough plane.

The size of the short-term memory is controlled by the beam width at passing range x_p that determines the number of data N. Larger memory sizes can include interferring echoes from other objects. Another limit on memory size is the expected length over which the piecewise linear trajectory is valid. A sonar that moves more erratically would produce coincidence over a smaller number of successive echoes.

Maximizing the peak of the sum of the short-term memory columns was the method used as a stopping rule for object perception, and it seems to work well. We also plan to investigate the product the column terms. Since the terms are generates as histograms, this product would be similar to a maximum-likelihood estimate.

We assume that the sonar orientation θ_s is constant, which is a form of minimum energy constraint. If more data from a reflector is needed, θ_s can increase and more echoes can be observed as the sonar passes the object, but at additional energy expense. We assume that biosonars can classify landmarks from N readings.

6. Conclusions

This paper has presented a non-linear processing method using data selection (strong echoes), histograms and thresholds to classify objects with a moving sonar. Our sonar generates a random PAP sequence related to echo waveform amplitude. Neuromorphic elements, such as delays, threshold, coincidence detection, short-term memory, and massive parallelism can classify certain objects from their echoes. When the sonar moves along a linear trajectory, a small object produces hyperbolic range readings parameterized by the passing range. Estimates of the passing range form a coincidence of values that can be detected from the sum of the columns in short-term memory. This talk demonstrates that features of range and passing-range data are useful for object classification.

7. References

[1] R. Kuc, M. Kirichenko and M. Lepekha. Adaptive and mobile biomimetic sonar recognizes objects from echoes. *Oceans'99.*

[2] N. Kirichenko, R. Kuc, and N. Lepekha. 3-D object detection with ultrasonic echo-signals. *Problems of Control and Informatics*, 5, 110-122. 1999.

[3] R. Kuc. Recognizing retro-reflectors with an obliquely-oriented multi-point sonar and acoustic flow. *International Journal of Robotics Research*, 22(2):129–145, 2003.

[4] R. Kuc. Neuro-computational processing of moving sonar echoes classifies and localizes foliage. *J. Acoust. Soc. Amer*, 116(3):1811-1818, 2004.